The 3p valence photoelectron spectrum of Ar clusters

Uwe Hergenhahn,* Silko Barth, Volker Ulrich,
Melanie Mucke, Sanjeev Joshi, and Toralf Lischke
Max-Planck-Institut für Plasmaphysik, EURATOM Association,
Boltzmannstr. 2, 85748 Garching, Germany

Andreas Lindblad, Torbjörn Rander, Gunnar Öhrwall, and Olle Björneholm
Department of Physics and Materials Science,
Uppsala University, Box 530, SE-751 21 Uppsala, Sweden

(Dated: June 17, 2010)

Abstract

The shape of the outer valence (3p) photoelectron spectrum of Ar clusters is investigated by vacuum ultraviolet photoionization with synchrotron radiation. We show the dependence of the spectrum on cluster size, and the change of its shape with photon energy. Inelastic losses due to intracluster photoelectron scattering are most important for changes in the photoelectron main line, and explain the appearance of additional peaks. A comparison of our results to earlier work on bulk condensed Ar and Ar thin films is given. Evidence for a deviation of the photoionization cross sections for clusters from the atomic ones has not been found.

PACS numbers: 36.40.Cg, 36.40.Mr, 61.46.Bc

v2, Table I corrected

*uwe.hergenhahn@ipp.mpg.de; Mail address: IPP, c/o Helmholtz-Zentrum Berlin, Albert-Einstein-Str. 15, 12489 Berlin, Germany

I. INTRODUCTION

One of the main motives in the study of clusters is to see how properties of the infinitely extended bulk develop from the isolated atom or molecule. In such studies, the rare gas clusters have become popular sample systems, as they are comparatively easy to produce in different sizes. With respect to their physics, they are prototypes of ideal insulators. In this article, we will be concerned with the electronic structure of small to medium-sized Ar clusters, as observed by photoionization of the outer valence ($3p$) band.

A number of effects cause the photoelectron spectra from Ar clusters, or bulk Ar produced by condensation, to be different from the isolated atom. Already in a system as small as the Ar dimer, the ionization potential differs markedly from that of the isolated atom. This in first place is a final state effect, as the Ar dimer cation possesses some bound states [1–3]. For clusters growing to about thirty atoms, from mass resolved appearance energy measurements also an influence of initial state effects was suggested [4, 5]. These experiments were detailed, but did not yield insight to properties of the electronic structure beyond the position of the ionization potential (IP), or the vacuum level in a solid state terminology. The full shape of the outer valence photoelectron spectrum of Ar clusters was shown in works by Carnovale *et al.* [6] at the photon energy of the He Iα line (21.2 eV), and in a comparative study of several electronic subshells of Ar, Kr and Xe clusters by Feifel *et al.* [7].

An important characteristic believed to be general for rare gas cluster photoelectron spectra is the higher binding energy of electrons emerging from the cluster surface compared to ones from the cluster interior (surface-bulk splitting). This is interpreted as a final state effect caused by polarization screening of the medium surrounding the positively charged vacancy. This effect, plus spin-orbit splitting, is sufficient to explain most inner valence and core level spectra of rare gas clusters [7], but fails to explain the structure seen in outer valence photoionization spectra. The interpretation of the latter therefore remained qualitative and concentrated on their gross structure. Carnovale *et al.* tried to put forward a chromophore model, which predicts production of an Ar_{13}^{+} unit (a single atom surrounded by one full, icosahedric shell) as a result of the ionization.

Photoelectron spectra of bulk condensed Ar were first measured by Schwentner *et al.* [8], and were intensively discussed later on [9–13].

In this work, we attempt to shed further light on the interpretation of the Ar cluster

band structure by showing and analyzing spectra measured at different cluster sizes and photon energies. Of particular importance will be the discussion of inelastic loss effects. This mechanism, which results in the creation of an exciton by scattering of a valence photoelectron at a different site within the same cluster, has been investigated earlier by measuring the resulting satellite (or electron loss) spectrum [9, 14, 15]. Here we will show how this effect is reflected in the main line spectrum.

II. EXPERIMENTAL

Photoelectron spectra were measured at the third generation synchrotron radiation source BESSY (Berlin, Germany). We compile results of various beamtimes at two undulator beamlines. An energy dependent series of medium-sized Ar clusters and the $3p$, $3s$ comparison were recorded at the U125/1 PGM beamline [16]. The spectra of larger clusters and some additional measurements were carried out later at the newly constructed UE112/lowE PGMa beamline [17]. In all cases, horizontally linearly polarized radiation was used.

The apparatus for production of a cluster jet and for recording the photoelectron spectra has been described in detail earlier [18, 19], and only a brief outline shall be given here. Clusters are produced by expansion of Ar gas through a liquid nitrogen cooled nozzle into an expansion chamber, which is separated from the main interaction chamber by a conical skimmer. The use of copper nozzles with a conical profile ensures good thermal properties and efficient condensation of the expanding gas. Knowing the nozzle temperature, its geometry and the stagnation pressure the mean size of the clusters N can be estimated from empirically derived scaling laws, which are used here in a formulation due to Hagena [20] (see also [21]). All relevant parameters are collected in Table I. The use of scaling laws to determine the size distribution of noble gas clusters has recently been critically revisited by Bergersen *et al.* [22]. We will comment on this topic below.

Photoelectrons produced by interaction of the synchrotron radiation with the cluster jet were detected in a hemispherical electron analyzer (Scienta ES 200) mounted in the dipole plane under the 'magic angle' of 54.7° to the horizontal. Within the dipole approximation, in this geometry differential cross sections are proportional to the total cross sections for the respective processes.

The Ar $3p$ spectra of medium-sized clusters, from which results shown in Fig.s 1, 3, 4

and 5 were derived, have been recorded at an analyzer pass energy of 20 eV, an analyzer slit setting of 500 μm, and a constant beamline exit slit of 410 μm. Dependent on the photon energy, this leads to a total apparatus broadening of 60–100 meV. We have observed a non-linear behavior of the measured vs. the true count rate, as described for a similar electron analyzer in Ref. [23]. An intensity calibration series was therefore used to compensate for this effect. The kinetic energy dependence of the analyzer transmission function was determined by recording the areas of Ne $2s$ atomic photoelectron lines, and normalizing them to the literature cross section [24] and the flux curve of the beamline as recorded with a GaAs photodiode. As this method relies on an external monitor it is less accurate than more tedious procedures based on electron spectra alone [25], but here we only use it for correcting the change in transmission along the $3p$ atomic and cluster lines within one energy. To further isolate effects of inelastic electron scattering spectra of the Ar $3p$ and $3s$ main lines were recorded subsequently and at identical kinetic energies, at a pass energy of 40 eV and with an approx. total energy resolution of 90 meV.

Additional spectra of larger Ar clusters were recorded independently with a pass energy of 5 eV and an approx. total apparatus energy resolution of 20 meV. Here, the transmission function of the analyser was determined from the area of the atomic Ar $3p_{1/2}$ photoline, normalized to the atomic $3p$ cross section and the beamline flux as measured with a GaAs photodiode of known quantum efficiency. A spectrum of the excitonic satellite region was recorded at a pass energy of 20 eV and with a total apparatus resolution of 40 meV. No transmission correction was carried out for this spectrum.

Spectra shown vs. binding energy were calibrated to the known ionization energies of the atomic $3p$ levels, being 15.760 and 15.937 eV [26], and $3s$ level (29.23 eV [27]) respectively.

III. RESULTS

The $3p$ photoelectron spectra of medium-sized clusters at a number of kinetic energies are displayed in Fig. 1. The two spin-orbit split components of the atomic $3p$ photoelectron lines, resulting from the presence of uncondensed Ar gas in the jet, can be seen at the r.h.s. of the figure. We attribute the remainder of the spectrum to photoionization of Ar clusters. Within the cluster-related part of the spectrum, neither a spin-orbit splitting of two components nor a bulk-surface splitting due to differences in final state screening is

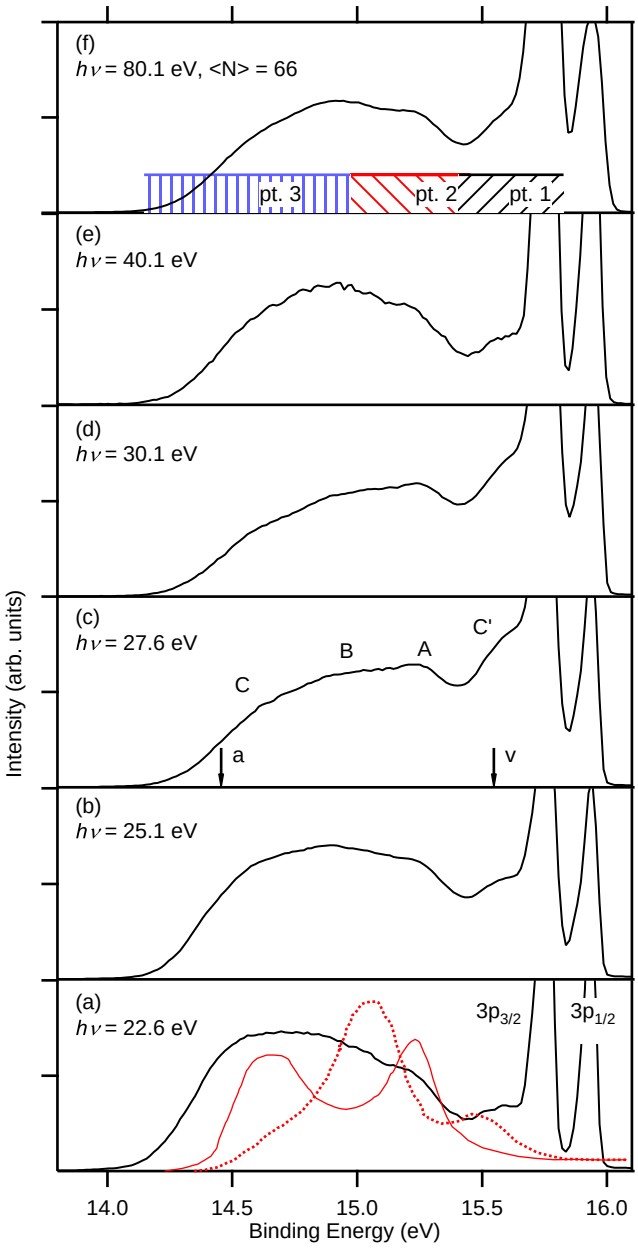

FIG. 1: (Color online) Photon energy dependence of the $3p$ photoelectron spectrum of medium-sized Ar clusters ($\langle N \rangle = 66$). The photoelectron lines from uncondensed monomers are designated. The different widths of the latter reflects the photon energy dependence of the beamline resolution at fixed exit slit width. The spectrum at 80.1 eV was repeatedly taken for reference purposes, and an average over all acquisitions is shown. Spectra have been normalized to equal total area. The photon energy behavior of the three regions designated in the top-most panel is further discussed below (Fig. 5). Letters A–C' in the middle panel follow the designations by Carnovale *et al.* [6], while arrows marked with 'a' and 'v', resp., designate the adiabatic and the vertical ionization potential of the Ar dimer in its ground state [1, 3]. In the bottom panel additional photoelectron spectra of an Ar monolayer for emission along the surface normal (thin solid line) and under an angle of $\theta = 40°$ (dotted line) with respect to the normal are shown [13].

TABLE I: Expansion parameters relevant for cluster size estimation (d: nozzle diameter, α: nozzle half opening angle, p: stagnation pressure, T: nozzle temperature, $\langle N \rangle$: expectation value of cluster size) (see text for details)

	Fig.s 1, 4, 5	*Fig.* 2	*Fig.* 3	*Fig.* 6
d (μm)	80	50	50	80
α (°)	15	15	15	15
p (mbar)	192	1010	1630	340
T (K)	81	93	95	85
$\langle N \rangle$	66	600	1670	195

immediately apparent. The shape of our spectra is consistent with experiments at two isolated photon energies (21.2 eV and 61 eV) reported in the literature [6, 7]. Here however, we display the development of the spectral structure at a number of photon energies in a consistent manner. Going from low to high kinetic energies, the most obvious changes are a reduction in the lowest binding energy part of the spectrum and an increase of the cluster photoelectron intensity at the low kinetic energy side next to the Ar $3p_{3/2}$ line at selected energies (panels c, d). We will discuss the former effect first.

It seems plausible to surmise an influence of intracluster photoelectron scattering in these spectra. In principle, such scattering processes can be elastic or inelastic. Elastic intracluster scattering has been observed in the angular distribution function of core level photoelectrons, referred to the polarization direction of the ionizing radiation [29, 30]. Due to properties of the quantum mechanical transition amplitudes, these functions can be quite anisotropic in the atomic case (peaking along or perpendicular to the polarization direction). For clusters this trend is partially blurred due to scattering, such that the angular distributions tend to be more isotropic. By definition, the energy spectrum does not change. In contrast to that, inelastic scattering leads to the appearance of additional structure in the photoelectron spectrum. Simple estimates using the mean free path of electrons in solid Ar [9] and of the sample density in the interaction region show that intracluster single scattering is the most probable process. In comparison, intercluster scattering (scattering of an electron from cluster X at cluster Y) is negligible. In the case of intracluster single scattering, additional features of well-defined energy can be produced, and have indeed been observed in earlier

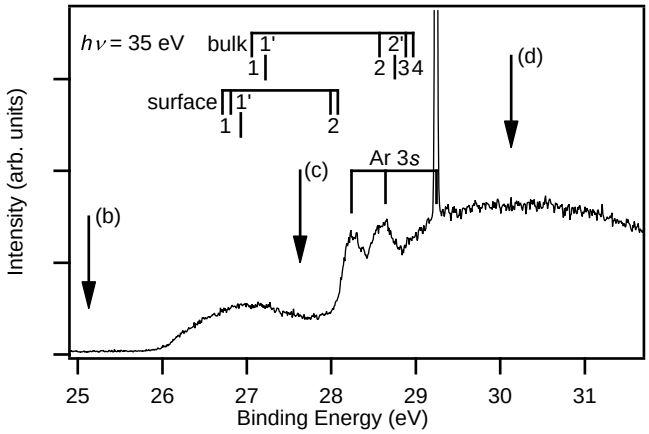

FIG. 2: Photoelectron spectrum of Ar clusters taken at 35 eV photon energy and showing the energy region of satellites pertaining to inelastic scattering of $3p$ photoelectrons. Energies designated by letters relate the binding energy axis to the panels in Fig.s 1 and 3. The Ar $3s$ main lines, coincidentally overlapping in energy, are designated (two broader features from cluster bulk and surface states, one sharp line from monomers). The energies of surface and bulk excitons known from optical absorption measurements of bulk condensed Ar, and shifted by 15.0 eV, are marked as well [28]. We attribute the remaining structure to interband transitions excited by $3p$ photoelectron scattering (see text for details).

experiments probing clusters in a similar regime [15].

A spectrum of $3p$ photoelectrons, which have undergone an energy loss due to inelastic scattering, is displayed in Fig. 2. We observe the onset of inelastic losses at a binding energy of 26.0 eV ($\pm$ 50 meV), or 12.0 eV when referred to the low binding energy flank of the $3p$ line (14.0 eV). This agrees excellently with earlier, lower resolution work [15]. The maximum of the first excitonic satellite occurs at a binding energy of 27.0 eV.

As can be seen in Fig. 2, inelastic losses start to play a role at photon energies in-between panels (b) and (c) in Fig. 1. In 1(c), a significant intensity loss of the least strongly bound parts of the cluster photoelectron line is seen. If we conjecture that it is the intensity of the excitonic features which is missing in the main line spectrum, we can conclude that part C of the spectrum, which is influenced by the intensity loss, pertains to bulk states, as inelastic scattering will be more important for them than for surface states.

We can corroborate this interpretation by additional observations: In Fig. 3, we compare the behavior of the cluster $3p$ band for two different cluster sizes. Inelastic losses in the

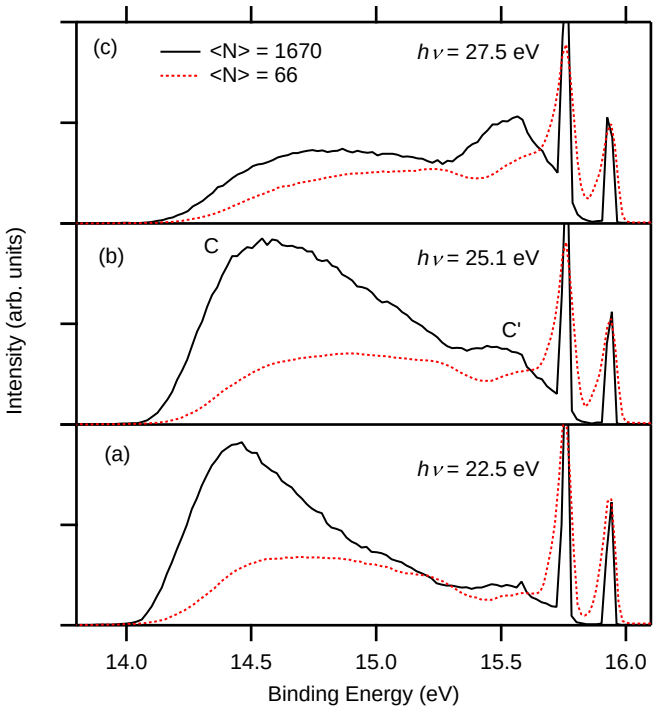

FIG. 3: (Color online) $3p$ photoelectron spectra of large Ar clusters ($\langle N \rangle = 1670$) at photon energies around the onset of inelastic losses. The spectra of ($\langle N \rangle = 66$) clusters given in Fig. 1 are repeated for comparison (dotted lines). Each set of three spectra was normalized to equal area of the atomic $3p_{1/2}$ photoline. A scaling constant between the two sets of data was chosen to allow for an easy comparison.

region identified with bulk photoionization are much stronger for the larger clusters, as can be expected.

We briefly return to the interpretation of Fig. 2. Comparisons with earlier observations of these loss structures can be made. Michaud and Sanche directly determined the energy loss spectrum of low (0–20 eV) kinetic energy electrons by passing a monoenergetic electron beam through a condensed multilayer Ar film [31]. The optical absorption of Ar films [28] as well as luminescence measurements of the electron impact created excitons in Ar films [32] and clusters [33] have also been reported. These investigations show more structure in the loss or absorption spectrum, respectively, than we observe. This is natural, as we implicitly average over all binding energies of the $3p$ photoelectrons. A detailed assignment of the structure between 12 and 14 eV energy loss to different excitonic features is given in [31], and will not be repeated here. The agreement of observed energies and gross structure

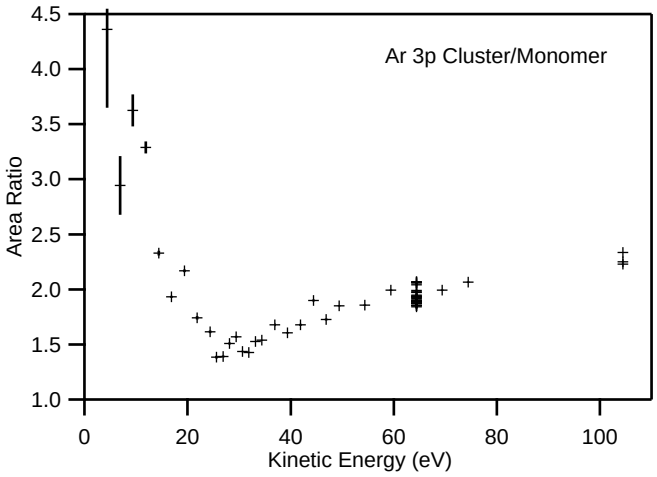

FIG. 4: Ratio of the $3p$ cluster feature divided by the $3p$ monomer feature, displayed vs. kinetic energy of the $3p_{3/2}$ atomic photoelectron line. (This can be considered a lower limit of the kinetic energy of the respective cluster photoelectrons.) The span of the data points at a kinetic energy of approx. 61.3 eV, which were repeatedly taken during acquisition of the data set, is indicative of the error due to variations of the cluster beam parameters with time. Error bars at low kinetic energy reflect uncertainty of the transmission function correction. Compared to that, the statistical error of the data is unimportant. See text for details.

of the loss features is excellent up to a binding energy of approx. 30 eV. At higher binding energies, interband transitions excited by scattering as well as satellite states can contribute to the signal. These structures have not been assigned in detail so far, but are outside the scope of this article. An indirect observation of the inelastic $3p$ scattering channels has also been made by zero-kinetic-energy electron, ion coincidence spectroscopy [34].

The wide range behavior of the total cluster photoelectron intensity of the data, which is partly shown in Fig. 1, has been determined relative to the atomic photoelectron intensity, and is displayed in Fig. 4. This curve is reminiscent of the universal loss curve well known for electron escape from bulk matter. We would like to note that the atomic Ar $3p$ photoelectron cross section undergoes a variation by a factor of 50 within the energy range shown, due to a Cooper minimum around a photon energy of 50 eV (35.4 eV in kinetic energy) [24]. One important finding from this work is that this atomic feature of the photoionization cross section occurs in clusters in much the same way. Generally, our results corroborate the use of atomic cross section for modeling of rare gas clusters in a radiation field.

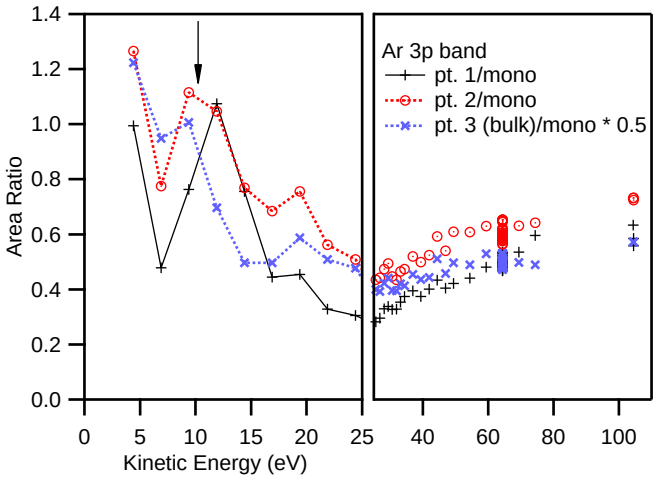

FIG. 5: (Color online) Ratio of three different regions within the $3p$ valence spectrum of ($\langle N \rangle = 66$) Ar clusters to the Ar $3p$ monomer lines, with regions as indicated in the top panel of Fig. 1. An enlarged view is displayed for low kinetic energies (left panel). As part 3 represents a wider energy interval than the other two regions, its values have been divided by two to allow for a better comparison. Some points have been connected to guide the eye. The arrow marks the onset of inelastic losses as seen in Fig. 2. Black symbols pertain to feature C' of Carnovale *et al.* [6], red symbols to A (with some overlap also with B), and blue symbols to B and C. The kinetic energy refers to the Ar $3p_{3/2}$ monomer line.

In order to give a more differentiated view of the kinetic energy dependent line structure changes we have divided the $3p$ valence spectrum into three different binding energy regions, as shown in the top panel of Fig. 1. The intensity of these regions relative to the total atomic photoionization cross section is presented in Fig. 5.

IV. DISCUSSION

The Ar dimer and its cation are well understood ([3] and Ref. therein). The ionized system has a much smaller bond length than the neutral, and the amount of energy required to dissociate it is much larger. By virtue of the Franck-Condon (FC) principle, photoionization creates a positively charged system at the nuclear geometry of the neutral, which is called a vertical transition. Therefore, the ground state of the cation cannot be reached by this technique. Combining the FC principle with quantum mechanics leads to a set of

transition probabilities between the initial state (here the neutral vibrational ground state) and vibrationally excited states of the positively charged system, which are calculated from the overlap of the respective nuclear wavefunctions ('FC factors'). From that, a considerable amount of nuclear energy is stored in the final state, which is experimentally seen from the huge difference between adiabatic and vertical ionization potential, marked 'a' and 'v' in panel (c) of Fig. 1.

Carnovale *et al.* [6] assigned labels A-C' to visibly distinguishable features of their He I spectrum (see Fig. 1). Further, they attempted to explain their origin in a molecular picture, by approximating the FC factors from a procedure, which graphically maps the ground state wavefunction into energy space by reflection on the ionized states' potential curve ('reflection principle', [37].) The energies of ionized states were calculated for some highly symmetric isomers of cationic Ar_N^+ clusters, with $N = 3, 7, 13$. Spin-orbit interaction was not taken into account, and agreement with the measured spectra was qualitative at best. Features C and C' were both assigned to an Ar_{13}^+ core ('chromophore'). We see, however, in Fig. 1 that these features have a different photon energy dependence.

Feifel *et al.* [7], on the other hand, suggested that the Ar $3p$ structure, observed in their work on large clusters and comparable to our Fig. 3, is composed of two spin-orbit split bands of different widths. It is then mainly the area below feature C' which is assigned to the $3p_{1/2}$ band, while the remainder would pertain to $3p_{3/2}$. This interpretation draws its plausibility mainly from an inspection of the outer valence bands of the series Xe-Kr-Ar clusters (see [7]). However, while in the other clusters the spin-orbit splitting clearly separates the two components, in Ar it has at most the same magnitude than the splitting between p states of different symmetries, $p_{x,y}$ and p_z. We will discuss this point below.

The density of states of a thick Ar layer has been measured by Jacobi and Rotermund [11]. Its shape is quite similar to the valence photoemission spectrum observed in this work for large clusters (Fig. 3c). When comparing the energies of the band given in Ref. [11] to our measurements, one has to take into account that these are given with respect to the vacuum level and thus the electron affinity of solid Ar should be subtracted. Reported values for this quantity range from 0.0(5) eV [35] via −0.25 eV [36] to −0.4 eV [8, 32]. If we choose the latter value, the low binding energy flank seen by Jacobi and Rotermund at 13.6 eV agrees perfectly with our measurement. The work of Schwentner *et al.* [8] on the photoelectron spectra of rare gas solids is in satisfactory agreement to our spectra, too.

Qualitatively, the shape of our large cluster spectrum also agrees with the density of states calculated by Bacalis *et al.* [38], although this work shows a more structured appearance with two peaks, split by approx. 1.3 eV (1/10 Ry). If reflected in the experiment at all, this would correspond to the spacing between C, C'. The total valence band width in their 'quasiparticle corrected' approach amounts to 1.9 eV, in good agreement with our experiment. Altogether, we conclude that the valence band structure seen in the spectra of our large clusters is close to the one of bulk solid Ar, as far as can be inferred from the presented experiments.

For the medium-sized clusters, it is important to know which amount of their spectra results from surface atoms. The size estimate from the expansion parameters is $\langle N \rangle = 66$. Clusters of this size consist of little more than two fully closed, icosahedric shells, with about 2/3 surface atoms in total. That is, the surface contribution is dominating, however its composition and spectral shape are not *a priori* known. Below we will present evidence that the cluster size estimated from the expansion conditions should be considered a lower limit for the actual cluster size in our experiment.

Electron spectra of condensed Ar monolayers were recorded on a number of substrates [10, 12, 13]. They show a two-peak structure, with a splitting of approx. 0.5–0.7 eV and a total width of 1 eV approx. A tight-binding calculation [10] has rationalized this structure as consisting of three bands, two of which are similar in energy for most $\mathbf{k}$ values. One interpretation of this structure is that crystal field splitting has lifted the degeneracy for the $j = 3/2, |m_j| = 3/2$ and the $|m_j| = 1/2$ states. How meaningful these labels are, can only be inferred from the eigenvector components of the tight-binding Hamiltonian. Therefore, some authors refer to these bands as $p_{x,y}$ and p_z derived, arguing that crystal field splitting would outweigh spin-orbit effects for Ar, as opposed to the heavier noble gases Kr and Xe [12, 13]. The dispersion of these bands (energy change with observation angle relative to the substrate surface) amounts to 0.3–0.5 eV [10, 13].

A comparison of these to our results has to take into account that due to the unordered nature of our sample contributions of all emission angles with respect to the cluster surface overlap in our spectra. Published spectra for an Ar monolayer taken at two different angles [13] with He Iα UV radiation (21.2 eV) are shown in the bottom panel of Fig. 1. The intensity normalization with respect to our spectra is arbitrary. For comparison, the high binding energy flank of the literature data, which were referred to the Fermi level, has been aligned with our data by an upward shift of 5.5 eV. One then finds that the weak structures

C', A and B are reflected in the surface photoemission spectra of an Ar film, while region C is composed of surface and bulk photoemission. This explanation seems appealing on the basis of the current data, but should be further substantiated by measuring high resolution spectra for additional cluster sizes.

The identification of feature C as bulk related is in agreement with the strong suppression of the former part of the spectrum by inelastic losses, and with the kinetic energy dependence of the relative intensities (Fig. 5), in which parts 1 and 2 are seen to ascend from the minimum at about 25 eV with a larger slope than part 3.

In Fig. 5 one further detail can be seen: At the first two data points above the exciton creation threshold the area ratio of part 1 is seen to have increased in relative intensity significantly compared to the other regions. This ratio corresponds to the most strongly bound energy region, referred to as feature C' in 1. Further inspection of Fig.s 1 and 3 shows that its intensity even increases in absolute terms. We would like to relate this finding to a desorption experiment on condensed Ar [39]. There, in the corresponding photon energy range a first maximum in the desorption yield of Ar^+ and Ar_2^+ was observed. This was explained by the creation and subsequent decay of states of the type Ar_2^{**}. In these excimers, two excitons have been created at neighboring atoms. These complexes form at the surface or travel to the surface of the rare gas solid, where the excited dimer desorbs from the lattice and an electron is ejected by autoionization. The occurrence of this mechanism in clusters would explain why an enhancement of a certain region of the spectrum is seen, and why it occurs in a region of high binding energy. Also, such effect would be confined to an interval of photon energies, which as well fits to our observation. Nevertheless, currently other mechanisms, i.e. energy dependent changes in the final state density of states cannot be ruled out as an alternative explanation of the data. Between 26.5 and 28.5 eV in photon energy, a number of $3s \rightarrow nl$ Rydberg resonances are located, which have been discussed in Ref.s [40, 41]. Autoionization of these excited states into $3p$ single vacancies could also change the photoionization profiles. However, the effects in our electron spectra seem to extend over a wider range of energies. Moreover, the $3p$ photoelectron intensity from clusters is not largely affected by the resonances.

Above we have discussed the influence of electron scattering on the shape of the observed Ar $3p$ valence band. It is also instructive to consider its influence on other spectral features. In Fig. 6 we display the $3p$ and the $3s$ structure of Ar clusters, recorded at equal expansion

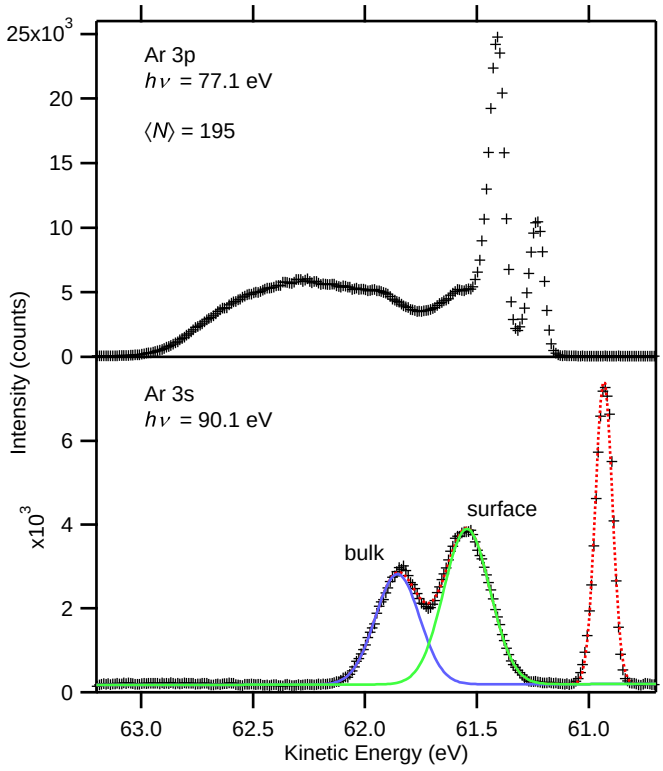

FIG. 6: (Color online) Ar 3s and 3p photoelectron lines recorded at equal kinetic energies. For the 3s line (bottom panel), the results of a least squares fit by Gaussian functions are shown (dotted: total, solid: bulk and surface component, not convoluted with apparatus broadening).

parameters and equal kinetic energies. Clearly distinct bulk and surface components of the 3s line are seen, the separation of which we find to be 0.31 eV. The surface/bulk intensity ratio is 1.47, inferred from the fit with Gaussian profiles which is shown in the figure. It is interesting that a linear interpolation between systems with three and four filled icosahedric shells and using this figure (1.47) leads to a cluster size of 205 atoms, in good agreement with a mean size of 195 derived from scaling laws. This however would imply that no losses due to inelastic scattering are influential on the bulk photoemission of 3s photoelectrons, opposing our results for 3p photoemission. We believe that this apparent contradiction likely occurs because the clusters under investigation in fact are larger than given by the scaling law. Earlier evidence for a systematic underestimation of rare gas cluster sizes by commonly used scaling laws has been compiled by Bergersen *et al.* [22].

During preparation of this work we learned of a study by Rolles *et al.* [42], in which angle resolved spectra are used to interpret the outer valence band structure of noble gas

clusters from Ar to Xe. As a general observation, these researchers see a decrease of the angular distribution parameter β from positive (but smaller than atomic) values at the high binding energy part of the spectrum towards isotropic values at lower binding energies. One obvious explanation is an influence of elastic scattering (or inelastic scattering with creation of phonons) on the angular distribution function of the emitted electron, which agrees with our interpretation of these features as bulk-related.

V. SUMMARY

We have presented a detailed interpretation of the outer valence band of Ar clusters, based on size and photon energy dependent photoelectron spectra. We find that the spectrum can be interpreted as a composite of bulk and surface related bands, with a broad, unstructured contribution from bulk and some characteristic features tentatively assigned to surface states. The spin-orbit splitting, which characterizes the atomic outer valence spectra of noble gases, and of the heavier noble gas clusters, is less important than crystal field effects in Ar. The gross behavior of the atomic $3p$ photoionization cross section, including its pronounced photon energy dependence due to a Cooper minimum, is reflected in the cluster cross section when an admittance for inelastic losses is made. A comparison of $3p$ and $3s$ bands of Ar clusters at equal expansion conditions suggests that the cluster size derived from the expansion conditions by popular scaling laws has to be considered a lower limit in this experiment.

Acknowledgments

UH would like to acknowledge useful discussions with Daniel Rolles, and communication of their work prior to publication. Thanks are due to Henrik Bergersen, Wandarad Pokapanich and Ioana Bradeanu for their help in data acquisition and to Karsten Horn for clarifying some aspects of the Ar thin film spectra. This work has partially been funded by the Deutsche Forschungsgemeinschaft and the Fonds der Chemischen Industrie. The Uppsala affiliated authors would like to acknowledge the support provided by the European Community - Research Infrastructure Action under the FP6 'Structuring the European Research Area' Programme (through the Integrated Infrastructure Initiative Integrating Activity on

Synchroton and Free Electron Laser Science - Contract R II 3-CT-2004-506008). In addition, the financial support from the Swedish Scientific Council (VR), the Swedish Foundation for Strategic Research (SSF) and the Knut and Alice Wallenbergs foundation are thankfully recognized.

---

[1] T. Pradeep, B. Niu, and D. A. Shirley, J. Chem. Phys. **98**, 5269 (1993).

[2] O. Echt, T. Fiegele, M. Rümmele, M. Probst, S. Matt-Leubner, J. Urban, P. Mach, J. Leszczynski, P. Scheier, and T. D. Märk, J. Chem. Phys. **123**, 084313 (2005).

[3] R. Signorell and F. Merkt, J. Chem. Phys. **109**, 9762 (1998).

[4] G. Ganteför, G. Bröker, E. Holub-Krappe, and A. Ding, J. Chem. Phys. **91**, 7972 (1989).

[5] W. Kamke, J. de Vries, J. Krauss, E. Kaiser, B. Kamke, and I. V. Hertel, Z. Phys. D **14**, 339 (1989).

[6] F. Carnovale, J. B. Peel, R. G. Rothwell, J. Valldorf, and P. J. Kuntz, J. Chem. Phys. **90**, 1452 (1989).

[7] R. Feifel, M. Tchaplyguine, G. Öhrwall, M. Salonen, M. Lundwall, R. R. T. Marinho, M. Gisselbrecht, S. L. Sorensen, A. Naves de Brito, L. Karlsson, N. Mårtensson, S. Svensson, and O. Björneholm, Eur. Phys. J. D **30**, 343 (2004).

[8] N. Schwentner, F.-J. Himpsel, V. Saile, M. Skibowski, W. Steinmann, and E. E. Koch, Phys. Rev. Lett. **34**, 528 (1975).

[9] N. Schwentner, Phys. Rev. B **14**, 5490 (1976).

[10] K. Kambe, Surf. Sci. **105**, 95 (1981).

[11] K. Jacobi and H. H. Rotermund, Surf. Sci. **116**, 435 (1982).

[12] K. Jacobi, Y. Hsu, and H. H. Rotermund, Surf. Sci. **114**, 683 (1982).

[13] K. Jacobi, Phys. Rev. B **38**, 5869 (1988).

[14] A. Knop, B. Wassermann, and E. Rühl, Phys. Rev. Lett. **80**, 2302 (1998).

[15] U. Hergenhahn, A. Kolmakov, M. Riedler, A. R. B. de Castro, O. Löfken, and T. Möller, Chem. Phys. Lett. **351**, 235 (2002).

[16] R. Follath, Nucl. Instrum. Methods A **467-468**, 418 (2001).

[17] R. Follath and J. S. Schmidt, Synchr. Rad. Instrum.: 8th Int. Conf., AIP Conference Proceedings **705**, ed. by T. Warwick *et al.* 631 (2004).

[18] S. P. Marburger, O. Kugeler, and U. Hergenhahn, Synchr. Rad. Instrum.: 8th Int. Conf., AIP Conference Proceedings **705**, ed. by T. Warwick *et al.* 1114 (2004).

[19] S. Barth, S. Joshi, S. Marburger, V. Ulrich, A. Lindblad, G. Öhrwall, O. Björneholm, and U. Hergenhahn, J. Chem. Phys. **122**, 241102 (2005).

[20] O. F. Hagena, Rev. Sci. Instrum. **63**, 2374 (1992).

[21] S. Barth, S. Marburger, O. Kugeler, V. Ulrich, S. Joshi, A. M. Bradshaw, and U. Hergenhahn, Chem. Phys. **329**, 246 (2006).

[22] H. Bergersen, M. Abu-samha, J. Harnes, O. Björneholm, S. Svensson, L. J. Sæthre, and K. J. Børve, Phys. Chem. Chem. Phys. **8**, 1891 (2006).

[23] N. Mannella, S. Marchesini, A. W. Kay, A. Nambu, T. Gresch, S.-H. Yang, B. S. Mun, J. M. Bussat, A. Rosenhahn, and C. S. Fadley, J. Electron Spectrosc. Relat. Phenom. **141**, 45 (2004).

[24] U. Becker and D. A. Shirley, in *VUV- and Soft X-Ray Photoionization*, edited by U. Becker and D. A. Shirley (Plenum Press, New York, 1996), p. 13.

[25] J. Jauhiainen, H. Aksela, O.-P. Sairanen, E. Nõmmiste, and S. Aksela, J. Phys. B. **29**, 3385 (1996).

[26] I. Velchev, W. Hogervorst, and W. Ubachs, J. Phys. B **32**, L511 (1999).

[27] M. E. Rudd, Y.-K. Kim, D. H. Madison, and T. J. Gay, Rev. Mod. Phys. **64**, 441 (1992).

[28] V. Saile, M. Skibowski, W. Steinmann, P. Gürtler, E. E. Koch, and A. Kozevnikov, Phys. Rev. Lett. **37**, 305 (1976).

[29] G. Öhrwall, M. Tchaplyguine, M. Gisselbrecht, M. Lundwall, R. Feifel, T. Rander, J. Schulz, R. R. T. Marinho, A. Lindgren, S. L. Sorensen, S. Svensson, and O. Björneholm, J. Phys. B **36**, 3937 (2003).

[30] H. Zhang, D. Rolles, Z. D. Pesic, J. D. Bozek, and N. Berrah, Phys. Rev. A **78**, 063201 (2008).

[31] M. Michaud and L. Sanche, Phys. Rev. B **50**, (1994) 4725.

[32] M. Runne and G. Zimmerer, Nucl. Instrum. Methods B **101**, 156 (1995).

[33] J. Wörmer, M. Joppien, G. Zimmerer, and T. Möller, Phys. Rev. Lett. **67**, 2053 (1991); J. Wörmer, R. Karnbach, M. Joppien, and T. Möller, J. Chem. Phys. **104**, 8269 (1996).

[34] J. de Vries, B. Kamke, H. Steger, B. Weisser, M. Honka, and W. Kamke, J. Chem. Phys. **101**, 2372 (1994).

[35] W. von Zdrojewski, J. G. Rabe, and W. F. Schmidt, Zeitschrift für Naturforschung A **35**, 672

(1980).

[36] W. Berthold, F. Rebentrost, P. Feulner, and U. Höfer, Appl. Phys. A **78**, 131 (2004).

[37] E. A. Gislason, J. Chem. Phys. **58**, 3702 (1973).

[38] N. C. Bacalis, D. A. Papaconstantopoulos, and W. E. Pickett, Phys. Rev. B **38**, 6218 (1988).

[39] Y. Baba, G. Dujardin, P. Feulner, and D. Menzel, Phys. Rev. Lett. **66**, 3269 (1991).

[40] A. A. Pavlychev and E. Rühl, J. Electron Spectrosc. Relat. Phenom. **106**, 207 (2000).

[41] H. Zhang, D. Rolles, J. D. Bozek, and N. Berrah, to be published.

[42] D. Rolles, H. Zhang, Z. D. Pesic, J. D. Bozek, and N. Berrah, Chem. Phys. Lett. **468**, 148 (2009).